The Mixed Mode I and II Interface Crack in Piezoelectromagneto–Elastic Anisotropic Bimaterials

R. Li
Post Doctoral Fellow

G. A. Kardomateas
Professor
e-mail: george.kardomateas@aerospace.gatech.edu

School of Aerospace Engineering,
Georgia Institute of Technology,
Atlanta, GA 30332-0150

Taking the electric–magnetic field inside the interface crack into account, the interface crack problem of dissimilar piezoelectromagneto (PEMO)–elastic anisotropic bimaterials under in-plane deformation is investigated. The conditions to decouple the in-plane and anti-plane deformation is presented for PEMO–elastic biaterials with a symmetry plane. Using the extended Stroh's dislocation theory of two-dimensional space and the analytic continuition principle of complex analysis, the interface crack problem is turned into a nonhomogeneous Hilbert equation in matrix notation. Four possible eigenvalues as well as four eigenvectors for the fundamental solution to the corresponding homogeneous Hilbert equation are found, so are four modes of singularities for the fields around the interface crack tip. These singularities are shown to have forms of $r^{-(1/2)\pm i\epsilon_1}$ *and* $r^{-(1/2)\pm i\epsilon_2}$*, in which the bimaterial constants* ϵ_1 *and* ϵ_2 *are proven to be real numbers for practical dissimilar PEMO–elastic bimaterials. Compared with the solution for the interface crack of dissimilar elastic bimaterials without electro–magnetic properties, two new additional singularities are discovered for the interface crack in the PEMO–elastic bimaterial media. The electric–magnetic field inside the crack is solved by employing the "energy method," which is based on finding the stationary point of the saddle surface of the energy release rate with respect to the electro–magnetic field inside the crack. Closed form expressions for the extended crack tip stress fields and crack open displacements are formulated, so are some other fracture characteristic parameters, such as the extended stress intensity factors and energy release rate* (G) *for dissimilar PEMO–elastic bimaterial solids. Finally, fundamental results and some conclusions are presented, which could have applications in the failure of piezoelectro/magneto–elastic devices.*
[DOI: 10.1115/1.2424468]

Keywords: piezoelectromagneto-elastic solids, dissimilar, anisotropic, interface crack, bimaterials

1 Introduction

The simultaneous presence of piezo-electric and piezo-magnetic material properties [1,2] usually lends a device some exceptional features such as converting energy from one form to the other form [3,4] and flat frequency responses [5]. These types of media find such applications in smart structure sensors, actuators, magnetoelectric memory apparatus, and broadband magnetic probes. In these applications, dissimilar bimaterials or layered composites are often incorporated. Having been considered as one of the common failure modes, an interface crack/delamination could be developed in structures made of piezoelectro magneto (PEMO)–elastic bimaterials, and then deteriorate the performance of the devices.

The interface crack phenomenon has been investigated for decades by many authors [6–13]. Morevover, although the piezo-magnetic material properties were not included, there are many studies on piezoelectric media or smart materials such as those by McMeeking [14], Kuo and Barnett [15] and Suo et al. [16]. In their studies, the singularities around the interface crack tip were found to be of the form $r^{-(1/2)\pm i\epsilon}$ and $r^{-(1/2)\pm\kappa}$, where ϵ and κ are real numbers. In particular, the paper by Suo et al. [16] has investigated this type of interface crack in detail.

As addressed in the literature (e.g., Refs. [2,4,5]), the simultaneous presence of the piezoelectric and piezomagnetic material properties usually have a big influence on the behavior of PEMO–elastic solids or layered structures. Thus, these piezoelectromagnetic material properties would also affect the interface fracture behavior of PEMO–elastic bimedia. Several papers on the study of cracks in monolithic PEMO–elastic solids are available such as Sih and Song [17], Song and Sih [18], and Gao et al. [19] etc. But few papers can be found for the problem of the interface crack in PEMO bimaterial solids. Gao et al. [20] presented a solution for a permeable interface crack and presented the singularities of the interface crack of the form as $r^{-(1/2)\pm i\epsilon_\alpha}$, but did not show whether ϵ_α are real or complex numbers. Furthermore, another important fracture parameter, the energy release rate G, has not been addressed in the literature for the in-plane interface crack of dissimilar anisotropic PEMO-elastic bimaterial solids.

In this research, the impermeable and permeable interface cracks in dissimilar PEMO bimaterial solids are investigated by employing the Stroh's dislocation theory [21], extended to PEMO–elastic media (e.g., Refs. [1,22]). The electric–magnetic field inside the crack is also considered. The Mode III interface crack solution has been analyzed in the authors' earlier work (Ref. [23]), and the current paper deals with the mixed mode I and II in-plane problems.

The paper is organized as follows: In Sec. 2, the conditions to decouple the in-plane and anti-plane deformations are derived and basic equations for the in-plane deformation are presented in the

Contributed by the Applied Mechanics Division of ASME for publication in the JOURNAL OF APPLIED MECHANICS. Manuscript received November 16, 2005; final manuscript received June 2, 2006. Review conducted by Zhigang Suo.

form of the extended Stroh's dislocation theory. In Sec. 3, a nonhomogenous Hilbert equation is obtained in matrix notation by using the analytic continuation principle of complex analysis. Four roots (i.e., four eigenvalues) to the corresponding homogenous Hilbert equation are found and so are four eigenvectors. Four possible singularities are then found in the form of $r^{-(1/2)\pm i\epsilon_1}$ and $r^{-(1/2)\pm i\epsilon_2}$. The bimaterial property constants ϵ_1 and ϵ_2 are proved to be real numbers for practical dissimilar bimaterial media. Compared with the solutions for conventional dissimilar bimaterials and piezoelectric bimaterials, two new types of singularities can be observed in this solution due to the simultaneous presence of piezoelectric and piezomagnetic material properties. Fracture parameters such as the extended stress intensity factor and the extended crack open displacement are presented in closed form for uniform applied remote loading.

The "energy method," which is based on finding the stationary point of the saddle surface of the energy release rate with respect to the electromagnetic field inside the crack [23] is employed to find the solution for the electric–magnetic fields inside the interface crack. Compact formulas for the energy release rate are derived for impermeable and permeable interface cracks. As a special solution, a crack in a monolithic anisotropic PEMO–elastic medium is also discussed by setting the upper and lower media identical. The conventional singularity of $r^{-(1/2)}$ is found for the crack tip fields in monolithic materials. This result is in good agreement with the results in the literature [18]. In Sec. 4, numerical results are presented to verify the characteristics of some bimaterial parameters and demonstrate the influence of the piezoelectromagnetic material properties on the energy release rate. The behavior of the energy release rate, G, is also studied under various loading conditions. In Sec. 5 we provide some useful conclusions.

2 Basic Equations

The basic equations, in extended Stroh's formalism, for PEMO–elastic material under generalized deformation are summarized in this section. The conditions to decouple the in-plane and anti-plane deformation are also discussed and some formulas are developed for the in-plane deformation.

In a fixed Cartesian coordinate system (x_1,x_2,x_3), the generalized Hooke's law for an elastic material considering both piezoelectric and piezomagnetic material properties may be written in the following form

$$\sigma_{ij} = c_{ijkl}u_{k,l} + e_{lij}\varphi^E_{,l} + \varrho_{lij}\varphi^H_{,l}$$

$$D_i = e_{ikl}u_{k,l} - \varepsilon_{il}\varphi^E_{,l} - \alpha_{il}\varphi^H_{,l}$$

$$B_i = \varrho_{ikl}u_{k,l} - \alpha_{li}\varphi^E_{,l} - \mu_{il}\varphi^H_{,l} \tag{1}$$

where i,j,k,l range in $\{1,2,3\}$ and the repeated indices imply summation; the comma stands for differentiation with respect to corresponding coordinate variables; σ_{ij} is the elastic stress, u_k the elastic displacement; c_{ijkl} the elastic moduli tensor; D_i the electric displacements; φ^E the electrostatic potential; ε_{il} the electric permittivity; B_i the magnetic induction (magnetic fluxes); φ^H the magnetic scalar potential; μ_{il} the magnetic permeability; and e_{ikl}, ϱ_{ikl}, and α_{li} the piezoelectric, piezomagnetic, and magnetoelectric coefficients, respectively. For the material constants, the following relationships hold

$$c_{ijkl} = c_{jikl} = c_{ijlk} = c_{klij}; \quad e_{ikl} = e_{ilk}; \quad \varrho_{ikl} = \varrho_{ilk}$$

$$\alpha_{il} = \alpha_{li}; \quad \varepsilon_{il} = \varepsilon_{li}; \quad \mu_{il} = \mu_{li} \tag{2}$$

The equilibrium equations read

$$\sigma_{ij,i} + f_j = 0, \quad D_{i,i} - f_e = 0, \quad B_{i,i} - f_m = 0 \tag{3}$$

If one defines the extended displacements as

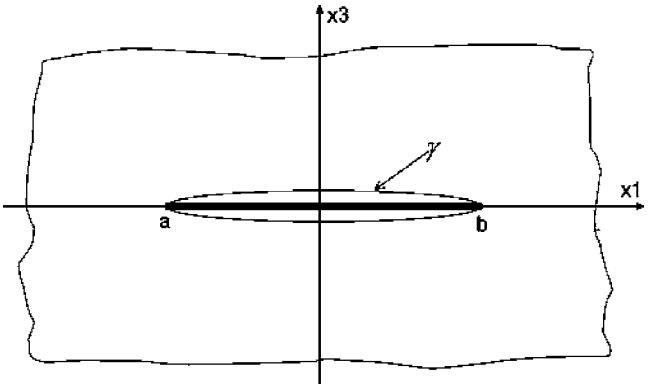

Fig. 1 An interface delamination between dissimilar piezoelectromagneto–elastic anisotropic bimedia and the associated contour integral path

$$U = [u_1, u_2, u_3, \varphi^E, \varphi^H]^T$$

or

$$U_K = u_k, \quad \text{for } K = 1,2,3; \quad U_4 = \varphi^E; \quad U_5 = \varphi^H \tag{4}$$

and, correspondingly, extends the conventional 3×3 stress tensor to a 3×5 stress tensor

$$\sigma_{iJ} = \sigma_{ij}, \quad \text{for } J = 1,2,3; \quad \sigma_{i4} = D_i; \quad \sigma_{i5} = B_i \tag{5}$$

then the equilibrium equations could be rewritten as

$$C_{iJKl}U_{K,li} + \mathbf{f}_J = 0 \tag{6}$$

where C_{iJKl} are the extended material constants

$$C_{iJKl} = \begin{cases} C_{ijkl} & J,\ K = 1,2,3 \\ e_{lJi} & J = 1,2,3;\ K = 4 \\ e_{iKl} & J = 4;\ K = 1,2,3 \\ \varrho_{lJi} & J = 1,2,3;\ K = 5 \\ \varrho_{iKl} & J = 5;\ K = 1,2,3 \\ -\alpha_{il} & J = 4,\ K = 5 \\ -\alpha_{li} & J = 5,\ K = 4 \\ -\varepsilon_{il} & J = K = 4 \\ -\mu_{il} & J = K = 5 \end{cases} \tag{7}$$

and $\mathbf{f}_J$ is the extended body force

$$\mathbf{f}_J = f_j, \quad \text{for } J = 1,2,3; \quad \mathbf{f}_4 = -f_e; \quad \mathbf{f}_5 = -f_m \tag{8}$$

in which, f_i, f_e, f_m are the body force, electric charge, and magnetic charge, respectively.

2.1 Decoupling the In-Plane and Anti-Plane Deformation. For a plane system, the extended displacement field depends on two variables, namely x_1 and x_3 (Fig. 1). Then, expanding the equilibrium Eq. (3) leads to the expressions

$$C_{1JK1}U_{K,11} + (C_{1JK3} + C_{3JK1})U_{K,13} + C_{3JK3}U_{K,33} = \mathbf{f_J}, \quad J,K = 1,\ldots,5 \tag{9}$$

Rewriting Eq. (9) gives

$$C_{1JK1}U_{K,11} + (C_{1JK3} + C_{3JK1})U_{K,13} + C_{3JK3}U_{K,33} + C_{1J21}U_{2,11} + (C_{1J23} + C_{3J21})U_{2,13} + C_{3J23}U_{2,33} = \mathbf{f_J}, \quad J,K = 1,3,4,5$$

$$C_{12K1}U_{K,11} + (C_{12K3} + C_{32K1})U_{K,13} + C_{32K3}U_{K,33} + C_{1221}U_{2,11} + (C_{1223} + C_{3221})U_{2,13} + C_{3223}U_{2,33} = \mathbf{f}_2, \quad K = 1,3,4,5 \tag{10}$$

To decouple the anti-plane and in-plane deformation, the coef-

ficients for the terms involving U_2 in Eq. $(10)_1$ and not involving U_2 in Eq. $(10)_2$ should vanish, leading to the following conditions

$$C_{1J21} = C_{1J23} = C_{3J21} = C_{3J23} = 0, \quad J = 1,3,4,5$$

$$C_{12K1} = C_{12K3} = C_{32K1} = C_{32K3} = 0, \quad K = 1,3,4,5 \tag{11}$$

or, in contracted form

$$C_{14} = C_{16} = C_{34} = C_{36} = C_{54} = C_{56} = 0$$

$$e_{16} = e_{14} = e_{36} = e_{34} = 0, \quad \varrho_{16} = \varrho_{14} = \varrho_{36} = \varrho_{34} = 0 \tag{12}$$

Equation $(12)_1$ is the condition which decouples the anti-plane and in-plane deformation for an anisotropic material with no piezoelectromagnetic properties. One may call it the mechanical decoupling condition. Unlike the conventional anisotropic media, one may see that if a PEMO–elastic material only satisfies this mechanical decoupling condition, the in-plane loading may still produce an anti-plane deformation, or vice versa.

2.2 Basic Equations for In-Plane Deformation. Since the anti-plane interface crack problem was studied by Li and Kardomateas [23], the current work focuses on the interface crack problem under in-plane deformation. The extended displacements Eq. (4) may be redefined as

$$U = [u_1, u_3, \varphi^E, \varphi^H]^T$$

or

$$U_1 = u_1, \quad U_2 = u_3, \quad U_3 = \varphi^E; \quad U_4 = \varphi^H \tag{13}$$

A nontrivial displacement solution to Eq. (6) with the corresponding stress function $\psi_k (k=1,2,3,4)$, in the absence of the extended body force, takes the form

$$U = \sum_{J=1}^{4} [\mathbf{a_J g_J(z_J)} + \bar{\mathbf{a}}_\mathbf{J} \bar{\mathbf{g}}_\mathbf{J}(\bar{\mathbf{z}}_\mathbf{J})], \quad \psi = \sum_{\mathbf{J=1}}^{\mathbf{4}} [\mathbf{b_J g_J(z_J)} + \bar{\mathbf{b}}_\mathbf{J} \bar{\mathbf{g}}_\mathbf{J}(\bar{\mathbf{z}}_\mathbf{J})],$$
$$\mathbf{z_J = x_1 + p_J x_3} \tag{14}$$

where $\bar{z}$ denotes the conjugate of a complex z; p_J is a complex number; $\mathbf{a}_j$ is a column vector; and $g(z_J)$ is a function vector to be determined from the boundary conditions.

The stresses can be written in term of a stress function, ψ, as

$$\sigma_{i1} = -\frac{\partial \psi_i}{\partial x_3}, \quad \sigma_{i3} = \frac{\partial \psi_i}{\partial x_1} \tag{15}$$

Substitution of Eq. (14) into Eq. (3) leads to the following eigenequation

$$[Q + p_J(R + R^T) + p_J^2 T]\mathbf{a}_J = 0 \tag{16}$$

where

$$Q_{JK} = C_{1JK1}, \quad R_{JK} = C_{1JK3}, \quad T_{JK} = C_{3JK3}, \quad J,K = 1,3,4,5 \tag{17}$$

Specifically, when contracted notation is employed, one has

$$[Q_{JK}] = \begin{bmatrix} c_{11} & c_{15} & e_{11} & \varrho_{11} \\ c_{15} & c_{55} & e_{15} & \varrho_{15} \\ e_{11} & e_{15} & -\varepsilon_{11} & -\alpha_{11} \\ \varrho_{11} & \varrho_{15} & -\alpha_{11} & -\mu_{11} \end{bmatrix}$$

$$[R_{JK}] = \begin{bmatrix} c_{15} & c_{13} & e_{31} & \varrho_{31} \\ c_{55} & c_{53} & e_{35} & \varrho_{35} \\ e_{15} & e_{13} & -\varepsilon_{13} & -\alpha_{13} \\ \varrho_{15} & \varrho_{13} & -\alpha_{31} & -\mu_{13} \end{bmatrix} \tag{18}$$

$$[T_{JK}] = \begin{bmatrix} c_{55} & c_{35} & e_{35} & \varrho_{35} \\ c_{35} & c_{33} & e_{33} & \varrho_{33} \\ e_{35} & e_{33} & -\varepsilon_{33} & -\alpha_{33} \\ \varrho_{35} & \varrho_{33} & -\alpha_{33} & -\mu_{33} \end{bmatrix} \tag{19}$$

As for the elastic and the piezoelectric cases (Suo et al. [16] and Lothe and Barnett [24]), it can be shown that the p_J are complex, and that if p_J is an eigenvalue of Eq. (16), then $\bar{p}_J$ is also an eigenvalue of Eq. (16) [1]. The roots p_J will be assumed to be all distinct, and in this paper equal roots are viewed as the limiting case of the distinct roots. From the relationship $\sigma_{13} = \sigma_{31}$, one may obtain

$$\mathbf{b}_J = (R^T + p_J T)\mathbf{a}_J = -\frac{1}{p_J}(Q + p_J R)\mathbf{a}_J \tag{20}$$

The combination of Eqs. (16) and (20) readily leads to

$$N \begin{bmatrix} \mathbf{a} \\ \mathbf{b} \end{bmatrix} = \begin{bmatrix} N_1 & N_2 \\ N_3 & N_1^T \end{bmatrix} \begin{bmatrix} \mathbf{a} \\ \mathbf{b} \end{bmatrix} = p \begin{bmatrix} \mathbf{a} \\ \mathbf{b} \end{bmatrix} \tag{21}$$

where N is an 8×8 matrix with $N_1 = -T^{-1}R^T$, $N_2 = T^{-1}$, $N_3 = RT^{-1}R^T - Q$; and the superscript T stands for the transpose of a matrix.

For the convenience of writing, we denote the extended traction vector on a surface $x_3 =$ constant, as

$$\mathbf{t} = [\sigma_{31}, \sigma_{33}, D_3, B_3]^T \tag{22}$$

Expression (14) may also be rewritten in vector form

$$\mathbf{u} = Ag(z_J) + \bar{A}\bar{g}(\bar{z}_J), \quad \psi = Bg(z_J) + \bar{B}\bar{g}(\bar{z}_J); \quad z_J = x_1 + p_J x_3 \tag{23}$$

where $A = [\mathbf{a}_1, \mathbf{a}_2, \mathbf{a}_3, \mathbf{a}_4]$, $B = [\mathbf{b}_1, \mathbf{b}_2, \mathbf{b}_3, \mathbf{b}_4]$, and $p_J (J = 1,2,3,4)$; these satisfy the orthogonality relations [25] after being properly normalized

$$\begin{bmatrix} B^T & A^T \\ \bar{B}^T & \bar{A}^T \end{bmatrix} \times \begin{bmatrix} A & \bar{A} \\ B & \bar{B} \end{bmatrix} = \begin{bmatrix} I & 0 \\ 0 & I \end{bmatrix} \tag{24}$$

Here, three useful matrices may be defined as

$$M = iAB^{-1}, \quad L = -2iBB^T, \quad S = i(2AB^T - I) \tag{25}$$

where $I = \mathrm{diag}[1,1,1,1]$ is the unit matrix. One can see from Eq. (24) that H and L are real and symmetric, whereas S and SL^{-1} are real and anti-symmetric. Moreover, the following relations can be verified.

$$M = L^{-1} + iL^{-1}S^T = L^{-1} - iSL^{-1} \tag{26}$$

which tells that M is Hermitian. The M matrix may be partitioned as

$$M = \begin{pmatrix} M_{11} & M_{13} & M_{14} \\ M_{31} & M_{33} & M_{34} \\ M_{41} & M_{43} & M_{44} \end{pmatrix} \tag{27}$$

where

$$M_{11} \sim [\text{elasticity}]^{-1}, \quad M_{33} \sim -[\text{permittivity}]^{-1}$$

$$M_{44} \sim -[\text{permeability}]^{-1}$$

$$M_{13} = \bar{M}_{31}^T \sim [\text{piezoelectricity}]^{-1} \tag{28}$$

$$M_{14} = \bar{M}_{41}^T \sim [\text{piezomagneticity}]^{-1}$$

$$M_{34} = \bar{M}_{43}^T \sim [\text{magnetoelectricity}]^{-1}$$

and M_{11} is positive definite [24], but $M_{33} < 0$ and $M_{44} < 0$.

If the coordinate system (x_1,x_2,x_3) transfers to a new coordinate system (x_1^*,x_2^*,x_3^*) by the in-plane rotation

$$\left[\frac{\partial x_i^*}{\partial x_j}\right]=\begin{bmatrix}\cos(\theta) & \sin(\theta) & 0\\ -\sin(\theta) & \cos(\theta) & 0\\ 0 & 0 & 1\end{bmatrix} \tag{29}$$

then one can easily show that

$$S(\theta)=\Omega^T(\theta)S\Omega(\theta),\quad L(\theta)=\Omega^T(\theta)L\Omega(\theta) \tag{30}$$

where

$$\Omega(\theta)=\begin{bmatrix}\cos(\theta) & \sin(\theta) & 0 & 0\\ -\sin(\theta) & \cos(\theta) & 0 & 0\\ 0 & 0 & 1 & 0\\ & & 0 & 0 & 0 & 1\end{bmatrix} \tag{31}$$

A transformation similar to Eq. (30) was also addressed in Suo et al. [16] in their fracture mechanics study of piezoelectric material.

3 Interface Cracks in PEMO-Elastic Bimaterial Media

3.1 Statement of the Problem. Let the medium I occupy the upper half space (denoted by L) and medium II be in the lower-half space (denoted by R); the interface crack is assumed to be located in the region $a<x_1<b$, $-\infty<x_2<\infty$ of the plane $x_3=0$ (Fig. 1). The $\sigma_{i3}^{\infty}=p^{\infty}=[\sigma_{13}^{\infty},\sigma_{33}^{\infty},D_3^{\infty},B_3^{\infty}]^T$ is applied at infinity. Under applied external loading, the crack may open and be filled with vacuum or air, in which an electric–magnetic field, denoted by D_3^0 and B_3^0, would be built up. This field is uniform if the applied loading σ_{i3}^{∞} is uniform [23]. By the superposition principle, this interface crack problem is equivalent to the one under the applied loading

$$p=[\sigma_{13}^{\infty},\ \sigma_{33}^{\infty},\ \Delta D_3^0,\ \Delta B_3^0]^T;\quad \Delta D_3^0=D_3^{\infty}-D_3^0,\quad \Delta B_3^0=B_3^{\infty}-B_3^0 \tag{32}$$

acting on the interface crack surfaces while the loading vanishes at infinity.

3.2 Formulation of the Solution to the Interface Crack. The procedure to derive the solution is similar to the one employed in Li and Kardomateas [26]. From Eq. (23), one can have the following expressions for this bimedia

$$U^{\mathrm{I}}=A_{\mathrm{I}}\phi_{\mathrm{I}}(z_J)+\bar{A}_{\mathrm{I}}\bar{\phi}_{\mathrm{I}}(\bar{z}_J)$$

$$\psi^{\mathrm{I}}=B_{\mathrm{I}}\phi_{\mathrm{I}}(z_J)+\bar{B}_{\mathrm{I}}\bar{\phi}_{\mathrm{I}}(\bar{z}_J) \tag{33}$$

where $U^{\mathrm{I}},\psi^{\mathrm{I}}$ are displacement and stress functions for $z_J\in L$; and for medium II

$$U^{\mathrm{II}}=A_{\mathrm{II}}\phi_{\mathrm{II}}(z_J)+\bar{A}_{\mathrm{II}}\bar{\phi}_{\mathrm{II}}(\bar{z}_J)$$

$$\psi^{\mathrm{II}}=B_{\mathrm{II}}\phi_{\mathrm{II}}(z_J)+\bar{B}_{\mathrm{II}}\bar{\phi}_{\mathrm{II}}(\bar{z}_J) \tag{34}$$

where $U^{\mathrm{II}},\psi^{\mathrm{II}}$ are displacement and stress functions for $z_J\in R$. For the convenience of writing, the symbols I and II, denoting the quantities in medium L and R, respectively, may be put as superscripts or subscripts.

Making use of Eq. $(15)_2$, the boundary condition for this problem can be written for the interface rack region $(a<x_1<b,x_3=0)$ as

$$\psi_+'^{\mathrm{I}}(x_1)=\psi_-'^{\mathrm{II}}(x_1)=-p(x_1) \tag{35}$$

and along the interface outside the crack ($x_1<a$ and $b<x_1$, $x_3=0$)

$$U_+^{\mathrm{I}}(x_1)=U_-^{\mathrm{II}}(x_1),\quad \psi_+'^{\mathrm{I}}(x_1)=\psi_-'^{\mathrm{II}}(x_1) \tag{36}$$

and at infinity

$$\sigma_{ij}^{\mathrm{I}}=\sigma_{ij}^{\mathrm{II}}=0,\quad \text{at infinity} \tag{37}$$

where the convention $\psi(x_1,x_3)=\psi_{\pm}(x_1)$ as $x_3\to 0^{\pm}$ for any function $\psi(x_1,x_3)$ was used and will be employed in the following sections.

The displacement continuity along the bonded interface gives

$$A_{\mathrm{I}}\phi_{\mathrm{I}+}(x_1)-\bar{A}_{\mathrm{II}}\bar{\phi}_{\mathrm{II}+}(x_1)=A_{\mathrm{II}}\phi_{\mathrm{II}-}(x_1)-\bar{A}_{\mathrm{I}}\bar{\phi}_{\mathrm{I}-}(x_1) \tag{38}$$

One may define a function

$$\Phi(z)=\begin{cases}A_{\mathrm{I}}\phi_{\mathrm{I}}(z)-\bar{A}_{\mathrm{II}}\bar{\phi}_{\mathrm{II}}(z), & z\in L\\ A_{\mathrm{II}}\phi_{\mathrm{II}}(z)-\bar{A}_{\mathrm{I}}\bar{\phi}_{\mathrm{I}}(z), & z\in R\end{cases} \tag{39}$$

which automatically satisfies the condition (38) and is analytic on the whole plane except the cut along the interface crack.

Differentiation of Eq. (39) yields

$$\Phi'(z)=\begin{cases}A_{\mathrm{I}}\phi_{\mathrm{I}}'(z)-\bar{A}_{\mathrm{II}}\bar{\phi}_{\mathrm{II}}'(z), & z\in L\\ A_{\mathrm{II}}\phi_{\mathrm{II}}'(z)-\bar{A}_{\mathrm{I}}\bar{\phi}_{\mathrm{I}}'(z), & z\in R\end{cases} \tag{40}$$

The traction continuity on the bonded interface leads to

$$B_{\mathrm{I}}\phi_{\mathrm{I}+}'(x_1)-\bar{B}_{\mathrm{II}}\bar{\phi}_{\mathrm{II}+}'(x_1)=B_{\mathrm{II}}\phi_{\mathrm{II}-}'(x_1)-\bar{B}_{\mathrm{I}}\bar{\phi}_{\mathrm{I}-}'(x_1) \tag{41}$$

Similarly to the displacement continuity, a function which automatically satisfies the condition Eq. (41) may be defined as

$$\omega(z)=\begin{cases}B_{\mathrm{I}}\phi_{\mathrm{I}}'(z)-\bar{B}_{\mathrm{II}}\bar{\phi}_{\mathrm{II}}'(z) & z\in L\\ B_{\mathrm{II}}\phi_{\mathrm{II}}'(z)-\bar{B}_{\mathrm{I}}\bar{\phi}_{\mathrm{I}}'(z), & z\in R\end{cases} \tag{42}$$

which is analytical on the whole plane except the cut along the interface crack.

Solving Eqs. (40) and (42) gives for $z\in L$

$$B_{\mathrm{I}}\phi_{\mathrm{I}}'(z)=N[i\Phi'(z)+\bar{M}_{\mathrm{II}}\omega(z)]$$

$$\bar{B}_{\mathrm{II}}\bar{\phi}_{\mathrm{II}}'(z)=B_{\mathrm{I}}\phi_{\mathrm{I}}'(z)-\omega(z) \tag{43}$$

and for $z\in R$

$$B_{\mathrm{II}}\phi_{\mathrm{II}}'(z)=\bar{N}[i\Phi'(z)+\bar{M}_{\mathrm{I}}\omega(z)]$$

$$\bar{B}_{\mathrm{I}}\bar{\phi}_{\mathrm{I}}'(z)=B_{\mathrm{II}}\phi_{\mathrm{II}}'(z)-\omega(z) \tag{44}$$

In the above equations, the following matrix was used

$$N^{-1}=M_{\mathrm{I}}+\bar{M}_{\mathrm{II}}=D+iW,\quad D=L_1^{-1}+L_2^{-1},\quad W=S_2L_2^{-1}-S_1L_1^{-1} \tag{45}$$

The matrix N is Hermitian since M_{I} and M_{II} are Hermitian; matrix D can be easily shown to be real symmetric and W to be real anti-symmetric.

Substituting Eqs. (43) and (44) into the boundary conditions Eqs. $(35)_{1,2}$, respectively, gives

$$B_{\mathrm{I}}\phi_{\mathrm{I}+}'(x_1)+B_{\mathrm{II}}\phi_{\mathrm{II}-}'(x_1)-\omega_-(x_1)=-p(x_1)$$

$$B_{\mathrm{II}}\phi_{\mathrm{II}-}'(x_1)+B_{\mathrm{I}}\phi_{\mathrm{I}+}'(x_1)-\omega_+(x_1)=-p(x_1) \tag{46}$$

Subtraction of Eq. $(46)_2$ from Eq. $(46)_1$ yields.

$$\omega_+(x_1)-\omega_-(x_1)=0 \tag{47}$$

which implies that $\omega(z)$ is continuous on the whole interface.

By the analytic continuation principle [27], the function $\omega(z)$ is analytical on the whole plane. But according to Liouville's theorem [27], this $\omega(z)$ must be a constant function in the whole domain. However, the condition in Eq. (37) imposes that this function vanish at infinity. Therefore, this constant function must be

identically zero in the whole plane, i.e.

$$\omega(z) = 0, \quad \text{for all } z \tag{48}$$

Then, either Eq. $(46)_1$ or Eq. $(46)_2$ leads to a general Hilbert equation in matrix notation

$$N\Phi'_+(x_1) + \bar{N}\Phi'_-(x_1) = ip(x_1), \quad a < x_1 < b \tag{49}$$

The homogenous equation corresponding to the above general Hilbert Eq. (49) can be written as

$$NX_+(x_1) + \bar{N}X_-(x_1) = 0, \quad a < x_1 < b \tag{50}$$

The following function vector may be considered as possible solution to Eq. (50)

$$\chi(z) = v(z-a)^{-\delta}(z-b)^{\delta-1} \tag{51}$$

which is analytic in the whole plane except the cut along (a,b) and has the property

$$z\chi(z) \to 1, \quad \text{as} \quad |z| \to \infty \tag{52}$$

Substitution of Eq. (51) into Eq. (50) leads to a 4×4 eigenvalue system

$$(N + e^{2\pi i\delta}\bar{N})v = 0, \quad \delta = 1/2 + i\epsilon \tag{53}$$

Since the procedure to obtain the solution to this eigenvalue problem (53) is significant for one to understand the singularities of the fields at the interface crack tip, a detailed study of Eq. (53) is presented in Appendix A, in which four possible eigenvalues of δ are found as

$$\delta_{1,2} = 1/2 \pm i\epsilon_1, \quad \delta_{3,4} = 1/2 \pm i\epsilon_2 \tag{54}$$

It is also shown in Appendix B that the bimaterial parameters ϵ_1 and ϵ_2 are real numbers and the corresponding four eigenvectors, $v_i (i=1\ldots4)$, are complex and satisfy the following conditions

$$v_2 = \bar{v}_1, \quad v_3 = \bar{v}_4 \tag{55}$$

The matrix defined as $\mathbf{v}=[v_1,v_2,v_3,v_4]$ can also be written as $\mathbf{v}=[v_1,\bar{v}_1,v_3\bar{v}_3]$.

Since N is a Hermitian matrix, the following identity can be readily verified

$$\bar{\mathbf{v}}^T N\mathbf{v} = \begin{bmatrix} \bar{v}_1^T N v_1 & 0 & 0 & 0 \\ 0 & v_1^T N \bar{v}_1 & 0 & 0 \\ 0 & 0 & \bar{v}_3^T N v_3 & 0 \\ 0 & 0 & 0 & v_3^T N \bar{v}_3 \end{bmatrix} \tag{56}$$

Denoting

$$\gamma_1 = \bar{v}_1^T N v_1, \quad \gamma_2 = v_1^T N \bar{v}_1, \quad \gamma_3 = \bar{v}_3^T N v_3, \quad \gamma_4 = v_3^T N \bar{v}_3 \tag{57}$$

then all the γs are real numbers, and $\gamma_1 \neq \gamma_2$, $\gamma_3 \neq \gamma_4$, unless N is real symmetric. One can further show

$$\gamma_1 = e^{2\pi\epsilon_1}\gamma_2 \quad \gamma_3 = e^{2\pi\epsilon_2}\gamma_4 \tag{58}$$

and normalize $\mathbf{v}$ as

$$\bar{\mathbf{v}}^T N\mathbf{v} = \text{diag}[\tilde{\gamma}_1 e^{\pi\epsilon_1}, \tilde{\gamma}_1 e^{-\pi\epsilon_1}, \tilde{\gamma}_2 e^{\pi\epsilon_2}, \tilde{\gamma}_2 e^{-\pi\epsilon_2}] \tag{59}$$

where $\tilde{\gamma}_1 = \gamma_1 e^{-\pi\epsilon_1}$ and $\tilde{\gamma}_2 = \gamma_3 e^{-\pi\epsilon_2}$ are real numbers.

Therefore, the fundamental solution to the homogeneous Hilbert Eq. (50) would take the form

$$X(z) = \frac{1}{\sqrt{(z-a)(z-b)}}\mathbf{v}\Delta(z;\epsilon_1,\epsilon_2) \tag{60}$$

$$\Delta(z;\epsilon_1,\epsilon_2) = \text{diag}\left[\left(\frac{z-b}{z-a}\right)^{i\epsilon_1}, \left(\frac{z-b}{z-a}\right)^{-i\epsilon_1}, \left(\frac{z-b}{z-a}\right)^{i\epsilon_2}, \left(\frac{z-b}{z-a}\right)^{-i\epsilon_2}\right]$$

One may see that there are four modes of singularities for the crack tip fields and these singularities have the following form

$$(x_1-a)^{-(1/2)\mp i\epsilon_1}(x_1-b)^{-(1/2)\pm i\epsilon_1}, \quad (x_1-a)^{-(1/2)\mp i\epsilon_2}(x_1-b)^{-(1/2)\pm i\epsilon_2} \tag{61}$$

Hence, a solution to the nonhomogeneous Hilbert Eq. (49), which vanishes at infinity, can be formulated as

$$\Phi'(z) = \frac{X(z)}{2\pi i}\int_{\overline{ab}} \frac{[X_+(x_1)]^{-1}N^{-1}[ip(x_1)]dx_1}{x_1 - z} \tag{62}$$

It can be seen that once the applied loading is given, a specific expression to Eq. (62) would be obtained, as would the displacement and stress functions.

For the applied constant loading $p(x_1)=p$, a closed form solution can be found by the contour integral method (Appendix B) as

$$\Phi'_p(z) = \mathbf{v}\left[I - \frac{\Delta(z;\epsilon_1,\epsilon_2)}{\sqrt{(z-a)(z-b)}}\Xi(z;\epsilon_1,\epsilon_2)\right]\mathbf{v}^{-1}[N+\bar{N}]^{-1}(ip) \tag{63}$$

where Ξ is defined as

$$\Xi(z;\epsilon_1,\epsilon_2) = \text{diag}\left[z_1 - \frac{(b+a)}{2} + (b-a)i\epsilon_1, z_2 - \frac{(b+a)}{2} - (b-a)i\epsilon_1, z_3 - \frac{(b+a)}{2} + (b-a)i\epsilon_2, z_4 - \frac{(b+a)}{2} - (b-a)i\epsilon_2\right] \tag{64}$$

Further integration of Eq. (63) leads to

$$\Phi_p(z) = \mathbf{v}[\Pi(z) - \sqrt{(z-a)(z-b)}\mathbf{\Delta}(z;\epsilon_1,\epsilon_2)]\mathbf{v}^{-1}[N+\bar{N}]^{-1}(ip) \tag{65}$$

where

$$\Pi(z) = \text{diag}[z_1, z_2, z_3, z_4] \tag{66}$$

and the terms contributing to rigid body motion have been omitted.

If we let r be the distance ahead of the crack tip, then, from expressions (63) and $(33)_2$ (or $(34)_2$), one can find that the crack tip fields, such as the extended stress field, can be expressed as the combination of

$$\sigma_{ij} \sim r^{-(1/2)\pm i\epsilon_1}, \quad r^{-(1/2)\pm i\epsilon_2} \tag{67}$$

i.e., a combination of four different singularities in piezomagnetoelectro–elastic dissimilar bimaterials. It should be mentioned that for conventional dissimilar bimedia, only two singularities of the form $r^{-(1/2)\pm i\epsilon}$ exist (ϵ is real [6]) and for the piezoelectric dissimilar bimaterials, four possible singularities of the form $r^{-(1/2)\pm i\epsilon}$ and $r^{-(1/2)\pm\kappa}$ were found (ϵ and κ are real [15,16]). In Eq. (67), two new singularities of the form $r^{-(1/2)\pm i\epsilon_2}$ (ϵ_2 is real) can be observed. These new types of singularities reflect the effects from the simultaneous presence of the piezoelectric and the piezomagnetic material properties.

3.3 Interface Crack Characteristic Parameters. With the solution to the stress functions in the foregoing section, some interesting fracture characteristic parameters such as the crack tip stress intensity factors and the extended displacements jump near the crack tip; furthermore, the energy release rate can be readily derived.

From Eqs. $(43)_1$ and $(43)_2$, the extended traction along the interface can be expressed as

$$\mathbf{t}(x_1) = Ni\Phi'_+(x_1) + \bar{N}i\Phi'_-(x_1) \tag{68}$$

We will show that the right hand side of Eq. (68) is real as required.

Substituting the stress function Eq. (63) into Eq. (68) leads to

$$\mathbf{t}(x_1) = -p + [NX_+(x_1) + \bar{N}X_-(x_1)]\Xi(x_1,\epsilon_1,\epsilon_2)(Nv + \bar{N}v)^{-1}p \tag{69}$$

or, when Eqs. (50) and (53) are employed, it reads

$$\mathbf{t}(x_1) = \begin{cases} -p + (N+\bar{N})v\dfrac{\Delta(x_1;\epsilon_1,\epsilon_2)\Xi(x_1;\epsilon_1,\epsilon_2)}{\sqrt{(x_1-a)(x_1-b)}}v^{-1}(N+\bar{N})^{-1}p & x_1 < a \text{ and } b < x_1 \\ -p & a < x_1 < b \end{cases} \tag{70}$$

Making use of Eqs. (56) and (59), the extended traction at a distance r ahead of the crack tip such as b (Fig. 1) can be expressed in the form

$$\begin{aligned}\mathbf{t}(r) = \frac{1}{\sqrt{2\pi r}}\sqrt{\pi(b-a)/2}(N+\bar{N})\Bigg[&\frac{(1/2+i\epsilon_1)r^{i\epsilon_1}}{(b-a)^{i\epsilon_1}\tilde{\gamma}_1\cosh(\pi\epsilon_1)}v_1\bar{v}^T{}_1p \\ &+\frac{(1/2-i\epsilon_1)r^{-i\epsilon_1}}{(b-a)^{-i\epsilon_1}\tilde{\gamma}_1\cosh(\pi\epsilon_1)}\bar{v}_1v_1^Tp \\ &+\frac{(1/2+i\epsilon_2)r^{i\epsilon_2}}{(b-a)^{i\epsilon_2}\tilde{\gamma}_2\cosh(\pi\epsilon_2)}v_3\bar{v}_3^Tp \\ &+\frac{(1/2-i\epsilon_2)r^{-i\epsilon_2}}{(b-a)^{-i\epsilon_2}\tilde{\gamma}_2\cosh(\pi\epsilon_2)}\bar{v}_3v_3^Tp\Bigg]\end{aligned} \tag{71}$$

where

$$p = [\sigma_{31}^{\infty}, \sigma_{33}^{\infty}, \Delta D_3^0, \Delta B_3^0]^T \tag{72}$$

One can easily see that the right side of Eq. (71) is a real vector, an expected result. The $v_i^Tp(i=1,3)$ are scalar (complex or real). Therefore, the interface traction ahead of the crack tip may be expressed in the space spanned by two eigenvectors (v_1, v_3) as

$$\begin{aligned}\mathbf{t}(r) = (N+\bar{N})\Bigg[&\frac{r^{i\epsilon_1}K_\sigma v_1}{\sqrt{2\pi r}\tilde{\gamma}_1\cosh^2(\epsilon_1\pi)} + \frac{r^{-i\epsilon_1}\bar{K}_\sigma\bar{v}_1}{\sqrt{2\pi r}\tilde{\gamma}_1\cosh^2(\epsilon_1\pi)} \\ &+\frac{r^{i\epsilon_2}K_{DB}v_3}{\sqrt{2\pi r}\tilde{\gamma}_2\cosh^2(\epsilon_2\pi)} + \frac{r^{-i\epsilon_2}\bar{K}_{DB}\bar{v}_3}{\sqrt{2\pi r}\tilde{\gamma}_2\cosh^2(\epsilon_2\pi)}\Bigg]\end{aligned} \tag{73}$$

where K_σ and K_{DB} are complex numbers, defined as

$$\begin{aligned}K_\sigma &= K_\mathrm{I} + iK_\mathrm{II} = \sqrt{\pi(b-a)/2}(1/2+i\epsilon_1)(b-a)^{-i\epsilon_1}\cosh(\epsilon_1\pi)\bar{v}_1^Tp \\ K_{DB} &= K_D + iK_B = \sqrt{\pi(b-a)/2}(1/2+i\epsilon_2)(b-a)^{-i\epsilon_2}\cosh(\epsilon_2\pi)\bar{v}_3^Tp\end{aligned} \tag{74}$$

These Ks can be called the extended stress intensity factors (ESIFs); similar notations have also been defined in the literature.

One can also extend the conventional crack open displacement (COD) to PEMO–electric materials. From Eqs. (33), (34), and (39), this extended crack open displacements (ECOD) can readily be evaluated by

$$\Delta\mathbf{u}(x_1) = \mathbf{u}_+^{\mathrm{I}}(x_1) - \mathbf{u}_-^{\mathrm{II}}(x_1) = \Phi_+(x_1) - \Phi_-(x_1) = \begin{cases} [(x_1-a)(b-x_1)]^{1/2}v[\Delta_+(x_1;\epsilon_1,\epsilon_2) + \Delta_-(x_1;\epsilon_1,\epsilon_2)]v^{-1}(N+\bar{N})^{-1}p, & a < x_1 < b \\ 0, & x_1 < a \text{ or } b < x_1 \end{cases} \tag{75}$$

Then the ECOD at a small distance r behind the tip of the interface crack reads

$$\begin{aligned}\Delta\mathbf{u}(r) = 2\sqrt{\frac{r}{2\pi}}\sqrt{\pi(b-a)/2}v\ \mathrm{diag}\Bigg[&\frac{r^{i\epsilon_1}}{(b-a)^{i\epsilon_1}\tilde{\gamma}_1}, \\ &\frac{r^{-i\epsilon_1}}{(b-a)^{-i\epsilon_1}\tilde{\gamma}_1}, \frac{r^{i\epsilon_2}}{(b-a)^{i\epsilon_2}\tilde{\gamma}_2}, \frac{r^{-i\epsilon_2}}{(b-a)^{-i\epsilon_2}\tilde{\gamma}_2}\Bigg]\bar{v}^Tp\end{aligned} \tag{76}$$

The ECOD can be further expressed in terms of the ESIF

$$\begin{aligned}\Delta\mathbf{u}(r) = 2\sqrt{\frac{r}{2\pi}}\Bigg[&\frac{r^{i\epsilon_1}K_\sigma v_1}{(1/2+i\epsilon_1)\tilde{\gamma}_1\cosh(\pi\epsilon_1)} \\ &+\frac{r^{-i\epsilon_1}\bar{K}_\sigma\bar{v}_1}{(1/2-i\epsilon_1)\tilde{\gamma}_1\cosh(\pi\epsilon_1)} + \frac{r^{i\epsilon_2}K_{DB}v_3}{(1/2+i\epsilon_2)\tilde{\gamma}_2\cosh(\pi\epsilon_2)} \\ &+\frac{r^{-i\epsilon_2}\bar{K}_{DB}\bar{v}_3}{(1/2-i\epsilon_2)\tilde{\gamma}_2\cosh(\pi\epsilon_2)}\Bigg]\end{aligned} \tag{77}$$

a real vector, as expected.

Next, the energy release rate G can be computed and it reads

$$\begin{aligned}G = \frac{1}{2}\lim_{\delta\to0^+}\frac{1}{\delta}\int_0^\delta \mathbf{t}(r)^T\Delta\mathbf{u}(\delta-r)dr &= \frac{\bar{v}_1^T(N+\bar{N})v_1}{2\tilde{\gamma}_1\cosh^4(\epsilon_1\pi)}|K_\sigma|^2 \\ &+\frac{v_1^T(N+\bar{N})\bar{v}_1}{2\tilde{\gamma}_1\cosh^4(\epsilon_1\pi)}|K_\sigma|^2 + \frac{v_3^T(N+\bar{N})\bar{v}_3}{2\tilde{\gamma}_2\cosh^4(\epsilon_2\pi)}|K_{DB}|^2 \\ &+\frac{\bar{v}_3^T(N+\bar{N})v_3}{2\tilde{\gamma}_2\cosh^4(\epsilon_2\pi)}|K_{DB}|^2\end{aligned} \tag{78}$$

In deriving Eq. (78), the following identity was employed

$$\begin{aligned}\lim_{\delta\to0^+}\frac{1}{\delta}\int_0^\delta r^{-(1/2)\pm i\epsilon}(\delta-r)^{(1/2)\mp i\epsilon}dr &= \int_0^1 s^{-(1/2)\pm i\epsilon}(1-s)^{(1/2)\mp i\epsilon}ds \\ &= (1/2\mp i\epsilon)\frac{\pi}{\cosh(\epsilon\pi)}\end{aligned} \tag{79}$$

Substituting Eq. (74) into Eq. (78), one can obtain

$$G = \frac{\pi(b-a)}{8} p^T H p \tag{80}$$

where

$$H = (1/2 + 2\epsilon_1^2)[\bar{v}_1\bar{v}_1^T(N+\bar{N})v_1v_1^T + v_1v_1^T(N+\bar{N})\bar{v}_1\bar{v}_1^T]/[\tilde{\gamma}_1^2\cosh^2(\epsilon_1\pi)] + (1/2 + 2\epsilon_2^2)[\bar{v}_3\bar{v}_3^T(N+\bar{N})v_3v_3^T + v_3v_3^T(N+\bar{N})\bar{v}_3\bar{v}_3^T]/[\tilde{\gamma}_2^2\cosh^2(\epsilon_2\pi)] \tag{81}$$

a symmetric real matrix.

All the formulas developed so far are functions of the unknown D_3^0 and B_3^0, the electric–magnetic field inside the interface crack. By finding the stationary point of the saddle surface of energy release rate with respect to the electromagnetic field inside the crack ("energy method" [23]), one can have the following equations in terms of D_3^0 and B_3^0

$$\frac{\partial G}{\partial D_3^0} = H_{13}\sigma_{31}^\infty + H_{23}\sigma_{33}^\infty + H_{33}\Delta D_3^0 + H_{34}\Delta B_3^0 = 0$$

$$\frac{\partial G}{\partial B_3^0} = H_{14}\sigma_{31}^\infty + H_{24}\sigma_{33}^\infty + H_{34}\Delta D_3^0 + H_{44}\Delta B_3^0 = 0 \tag{82}$$

which lead to

$$\Delta D_3^0 = D_3^\infty - D_3^0 = -\frac{H_{13}H_{44} - H_{14}H_{34}}{H_{33}H_{44} - H_{34}^2}\sigma_{13}^\infty - \frac{H_{23}H_{44} - H_{24}H_{34}}{H_{33}H_{44} - H_{34}^2}\sigma_{33}^\infty$$

$$\Delta B_3^0 = B_3^\infty - B_3^0 = -\frac{H_{14}H_{33} - H_{13}H_{34}}{H_{33}H_{44} - H_{34}^2}\sigma_{13}^\infty - \frac{H_{24}H_{33} - H_{23}H_{34}}{H_{33}H_{44} - H_{34}^2}\sigma_{33}^\infty \tag{83}$$

Then, the D_3^0 and B_3^0 can be calculated as

$$D_3^0 = D_3^\infty - \Delta D_3^0 = D_3^\infty - \frac{H_{14}H_{34} - H_{13}H_{44}}{H_{33}H_{44} - H_{34}^2}\sigma_{13}^\infty - \frac{H_{24}H_{34} - H_{23}H_{44}}{H_{33}H_{44} - H_{34}^2}\sigma_{33}^\infty$$

$$B_3^0 = B_3^\infty - \Delta B_3^0 = B_3^\infty - \frac{H_{13}H_{34} - H_{14}H_{33}}{H_{33}H_{44} - H_{34}^2}\sigma_{13}^\infty - \frac{H_{23}H_{34} - H_{24}H_{33}}{H_{33}H_{44} - H_{34}^2}\sigma_{33}^\infty \tag{84}$$

Now, one may further express the energy release rate in more explicit forms for two types of interface cracks: the impermeable and permeable interface cracks [14,16].

1. Impermeable interface crack, for which $D_3^0=0$ and $B_3^0=0$. The energy release rate reads

$$G_{\text{imp}} = \frac{\pi(b-a)}{8}[\sigma_{13}^\infty, \sigma_{33}^\infty, D_3^\infty, B_3^\infty] H [\sigma_{13}^\infty, \sigma_{33}^\infty, D_3^\infty, B_3^\infty]^T \tag{85}$$

2. Permeable interface crack, for which the electric–magnetic field, D_3^0 and B_3^0, inside the crack, is considered and given by Eq. (83). Substituting Eq. (83) into Eq. (80), one can obtain the energy release rate in a more explicit form as

$$G_{\text{perm}} = \frac{\pi(b-a)}{8}\left[\frac{\det(\tilde{H}_{22})}{\det(\hat{H})}(\sigma_{13}^\infty)^2 + \frac{\det(\tilde{H}_{12}+\tilde{H}_{21})}{\det(\hat{H})}(\sigma_{13}^\infty\sigma_{33}^\infty) + \frac{\det(\tilde{H}_{11})}{\det(\hat{H})}(\sigma_{33}^\infty)^2\right] \tag{86}$$

where, det( ) is the determinant of a square matrix; matrices $\tilde{H}_{\alpha\beta}$ $(\alpha,\beta=1,2)$ are the submatrices of H obtained by striking out the αth column and the βth row, and

$$\hat{H} = \begin{pmatrix} H_{33} & H_{34} \\ H_{43} & H_{44} \end{pmatrix} \tag{87}$$

In Eq. (86), one may clearly see that the applied mechanical loading σ_{13}^∞ and σ_{33}^∞ has a coupling effect on the energy release rate.

3.4 Special Case: A Crack in a Monolithic Piezoelectromagnetic Medium. As an illustration, this section will show that the solution to the Griffith type crack in monolithic piezomagnetoelectro–elastic solids can be conveniently obtained by setting the two media identical in the foregoing formulas of the interface crack problem. Specifically, the bimaterial matrix $D = L_1^{-1} + L_2^{-1} = 2L_1^{-1} = 2L_2^{-1} = 2L^{-1}$. Also, the N reduces to a 4×4 positive definite matrix, i.e.

$$N = \bar{N} = (2L^{-1})^{-1} = \tfrac{1}{2}L \tag{88}$$

The nonhomogenous Hilbert Eq. (49) then turns to

$$\Phi'_+(x_1) + \Phi'_-(x_1) = 2L^{-1}ip(x_1), \quad a < x_1 < b \tag{89}$$

A solution which vanishes at infinity is [26]

$$\Phi'(z) = \frac{1}{2\pi i}\,\text{diag}\left[\frac{1}{\sqrt{(z-a)(z-b)}}\right] \times \int_{\overline{ab}} \frac{\left\{\text{diag}\left[\frac{1}{\sqrt{(z-a)(z-b)}}\right]_+\right\}^{-1} L^{-1}[2ip(x_1)]dx_1}{x_1 - z} \tag{90}$$

If the applied loading is constant, then

$$\Phi'(z) = \text{diag}\left[1 - \frac{z-(a+b)/2}{\sqrt{(z-a)(z-b)}}\right] L^{-1}(ip) \tag{91}$$

Integrating Eq. (91), results in

$$\Phi(z) = \text{diag}[z - \sqrt{(z-a)(z-b)}]L^{-1}(ip) \tag{92}$$

where the constant contributing rigid body motion has been omitted.

Let

$$K = [K_{\text{II}},\ K_{\text{I}},\ K_D,\ K_B]^T \tag{93}$$

one then may easily show that the expression Eq. (93) becomes

$$K = \sqrt{\frac{\pi(b-a)}{2}}\,p \tag{94}$$

an interesting result that is similar in form to the conventional isotropic SIF. This result is also valid for some bimaterials with null bimaterial matrix W. Expressions (73) and (76) reduce, respectively, to.

$$\mathbf{t}(r) = \sqrt{\frac{1}{2\pi r}}K$$

and

Table 1 Properties of piezoelectromagneto–elastic bimaterial systems

		Medium II			
Properties	Medium I	(1)	(2)	(3)	(4)
c_{11} (GPa)	86.74	166.0	202.0	226.0	250.0
c_{13} (GPa)	27.15	78.0	105.0	124.0	142.7
c_{33} (GPa)	102.83	162.0	194.2	216.0	237.3
c_{35} (GPa)	68.81	43.0	43.7	44.0	44.6
e_{11} (c/m^2)	0.171	0.0	0.0	0.0	0.0
e_{13} (c/m^2)	−0.0187	0.0	0.0	0.0	0.0
e_{35} (c/m^2)	−0.0761	0.0	0.0	0.0	0.0
e_{31} (c/m^2)	0.0	−4.4	3.08	−2.2	−1.32
e_{33} (c/m^2)	0.0	18.6	13.02	9.3	5.58
e_{15} (c/m^2)	0.0	0.0	8.12	5.8	3.48
ρ_{15} (N/Am)	550	550.0	174.1	275.0	385.0
ρ_{31} (N/Am)	580.3	550.0	165.0	290.2	406.2
ρ_{33} (N/Am)	669.7	699.7	209.9	350.0	489.8
ε_{11} (c/Nm^2)	39.21×10^{-12}	11.2×10^{-10}	78.6×10^{-10}	56.4×10^{-10}	34.2×10^{-10}
ε_{13} (c/Nm^2)	0.86×10^{-12}	0.0	0.0	0.0	0.0
ε_{31} (c/Nm^2)	0.86×10^{-12}	0.0	0.0	0.0	0.0
ε_{33} (c/Nm^2)	40.42×10^{-12}	12.6×10^{-10}	88.5×10^{-10}	63.5×10^{-10}	38.5×10^{-10}
μ_{11} (Ns^2/C^2)	5.50×10^{-6}	5.0×10^{-6}	180.5×10^{-6}	297.0×10^{-6}	414.5×10^{-6}
μ_{33} (Ns^2/C^2)	10.0×10^{-6}	10.0×10^{-6}	541.0×10^{-6}	83.5×10^{-6}	112.9×10^{-6}

$$\Delta\mathbf{u}(r) = 4\sqrt{\frac{r}{2\pi}}L^{-1}K \tag{95}$$

Equations (95) can also be directly obtained from the functions (91) and (92).

Equation (95) shows that the crack tip field for the monolithic material is proportional to the inverse of the square root of r, i.e.

$$\sigma_{i_j} \sim \frac{1}{\sqrt{2\pi r}} \tag{96}$$

a result that is in agreement with the one obtained in Song and Sih [18].

The energy release rate reads as

$$G_0 = \frac{1}{2}K^T L^{-1}K = \frac{\pi(b-a)}{4}p^T L^{-1}p \tag{97}$$

which can also be obtained by substituting Eq. (95) into Eq. $(78)_1$.

4 Numerical Results and Discussion

The data for the piezoelectric and piezomagnetic properties of the upper and lower media of the dissimilar bimaterial systems are selected from the literature [4,18] and recorded in Table 1. The constituents of each of the bimaterial systems are PEMO—elastic materials.

Table 2 gives the results of some bimaterial parameters such as c_2 and c_4 [defined by Eq. (102)], $\beta_{1,2}$, and $\beta_{3,4}$ [defined by Eq. (103)]. One can see from these numerical results that c_2 and c_4 are larger than zero. $\beta_{1,2}$, $\beta_{3,4}$ are real numbers, and so are ϵ_1 and ϵ_2. These observations are in agreement with the results proved in Appendix A and show that four possible singularities of the form $r^{-(1/2)\pm i\epsilon_1}$ and $r^{-(1/2)\pm i\epsilon_2}$ with real ϵ_1 and ϵ_2 exist around the interface crack tip in PEMO–elastic bimaterials.

The results in Figs. 2 and 3 are used to demonstrate the influence of the bimaterial parameter c_2 on the energy release rate, G. These results show that the energy release rate increases as c_2 increases both for a permeable and an impermeable interface crack; the energy release rate of a permeable interface crack is larger than that of an impermeable interface crack if only the loading σ_{33} (far field tension normal to the crack) is applied (Fig. 2), while the energy release rate for a permeable interface crack is the same as that for an impermeable interface when the loading is only σ_{13} (far field in-plane shear, Fig. 3).

The bimaterial system Medium I—Medium II (1) (ϵ_1 =0.00950057, ϵ_2=0.00337206) will be used as an example in a further study to illustrate the energy release behavior of interface cracks in PEMO—elastic bimaterial solids.

Figure 4 plots the results of the energy release rate G of a permeable and an impermeable interface crack under any combination of loading σ_{33} and σ_{13}. It can be seen that the value of the energy release rate, G, for an interface crack, if considered as permeable, is larger than that of an interface crack if considered as impermeable, for any given pair of $(\sigma_{33}, \sigma_{13})$. Some details of this observation are shown in Figs. 5 and 6, where Fig. 5 is the variation of energy release rate versus the change of applied loading

Table 2 Bimaterial parameters

	Bimaterial systems			
Bimaterial parameters	Medium I–Medium II(1)	Medium I–Medium II(2)	Medium I–Medium II(3)	Medium I–Medium II(4)
c_2	2.0104×10^{-3}	2.4613×10^{-3}	5.1277×10^{-3}	7.5233×10^{-3}
c_4	1.6038×10^{-6}	5.5027×10^{-6}	7.6662×10^{-6}	1.01275×10^{-6}
$\beta_{1,2}$	±0.05976423	±0.05662615	±0.0971787	±0.11975132
$\beta_{3,4}$	±0.02119044	±0.04142584	±0.0284918	±0.02657485
ε_1	0.00950057	0.00900272	0.01541805	0.01896868
ε_2	0.00337206	0.00658936	0.00453338	0.00422852

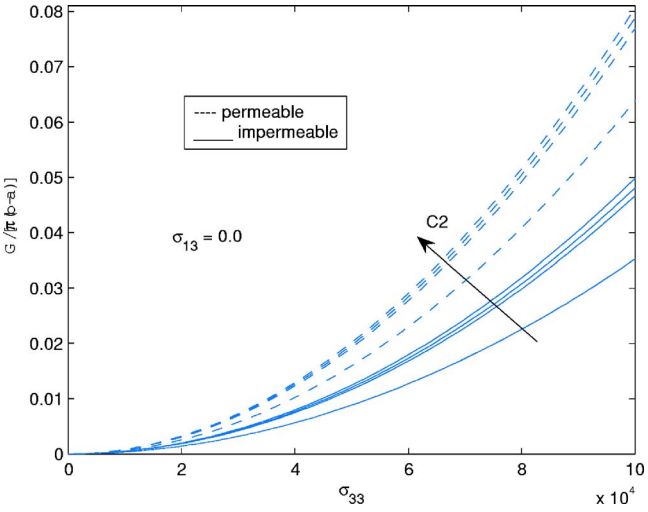

Fig. 2 Energy release rate versus bimaterial constant c_2 under pure mechanical loading σ_{33}

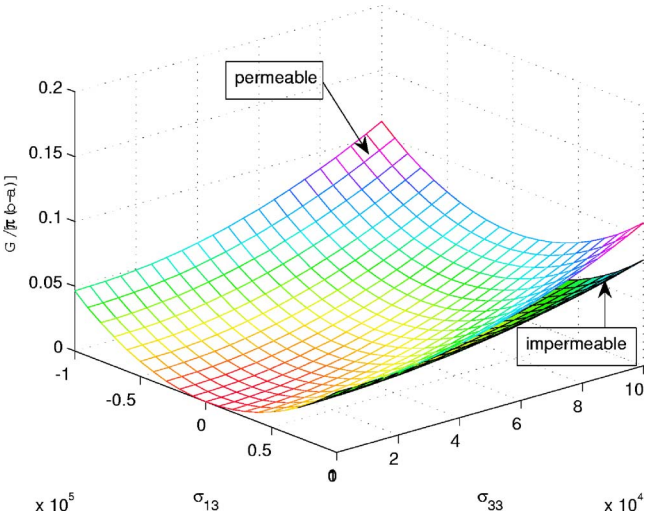

Fig. 4 Energy release rate for the combined mechanical loading σ_{13} and σ_{33}

σ_{33} for two given values of σ_{13}, and Fig. 6 is the variation of the energy release rate versus the change of applied loading σ_{13} for three given values of σ_{33}.

Figure 7 shows the results of energy release rate values for an impermeable interface crack under any combined electric–magnetic loading (D_3, B_3). An interesting phenomenon that can be seen here is that all the values of energy release rate G are less than or equal to zero. Negative energy release rates are physically impossible. This observation implies that a pure electric–magnetic loading (D_3, B_3) would be expected to retard the propagation of an interface crack in PEMO–elastic bimaterial systems. This retardation mechanism will be more clearly seen in the following discussions. Moreover, this retardation phenomenon has also been reported in the literature for cracks in monolithic electromagnetic materials [17].

Figures 8–11, respectively, demonstrate the influence of the applied electric or magnetic field on the energy release rate G under applied mechanical tensile loading σ_{33}. Figure 8 is the variation of G versus the applied loading σ_{33} for two given values of D_3 applied in different directions, namely, positive direction $(D_3 > 0)$ and negative direction $(D_3 < 0)$ and Fig. 9 is the variation of G versus any combination of loading (σ_{33}, D_3). Figure 10 is the G versus the applied loading σ_{33} for two given values of B_3 and Fig. 11 is G versus any combination of loading (σ_{33}, B_3). The results in Figs. 8 and 10 show that for a given D_3 or B_3, the applied mechanical loading σ_{33} has to exceed a certain value in order to reach a positive G. Here, we may call this value the thrust value, denoted as σ_{33}^{thr}.

Figures 8 and 10 also show that the values of the σ_{33}^{thr} are different for the applied D_3 or B_3 with the same amplitudes but different directions. One can see that the direction of applied D_3 or B_3 has an influence on the energy release rate, G. The influence of the direction of the electric or magnetic field can be viewed more clearly in Fig. 12, which shows the variation of G versus σ_{33} under the combined influence from a given (D_3, B_3). Here, a more subtle observation needs to be pointed out. The results in Fig. 7 show that the bigger the value of pure applied D_3 or/and B_3 is, the bigger a negative value G reaches. But this does not mean that the bigger value of applied D_3 or/and B_3 always makes the energy release rate G smaller (than the corresponding G with a smaller value of applied D_3 or/and B_3) when a mechanical loading is present. This can be easily verified from the results in Figs. 8 and

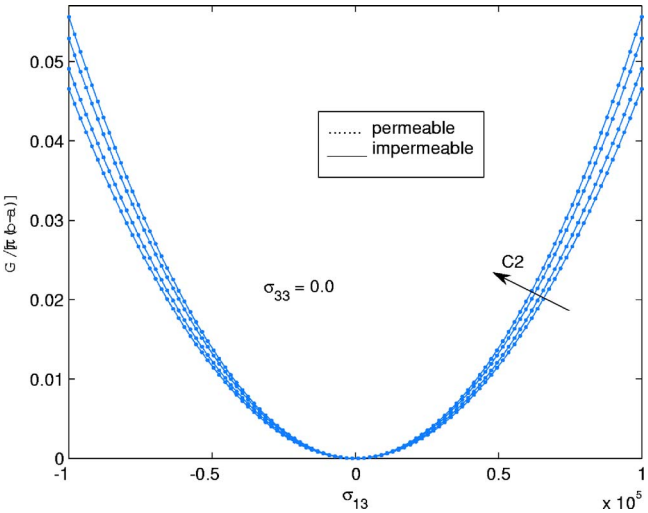

Fig. 3 Energy release rate versus bimaterial constant c_2 under pure mechanical loading σ_{13}

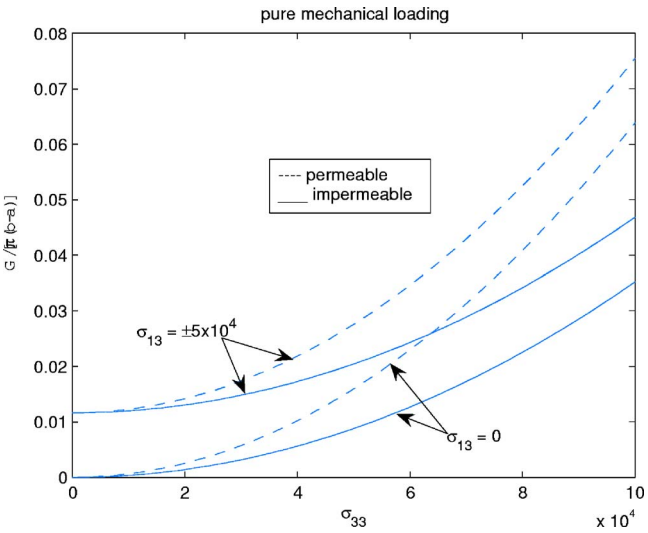

Fig. 5 Energy release rate versus σ_{33} for a given σ_{13}

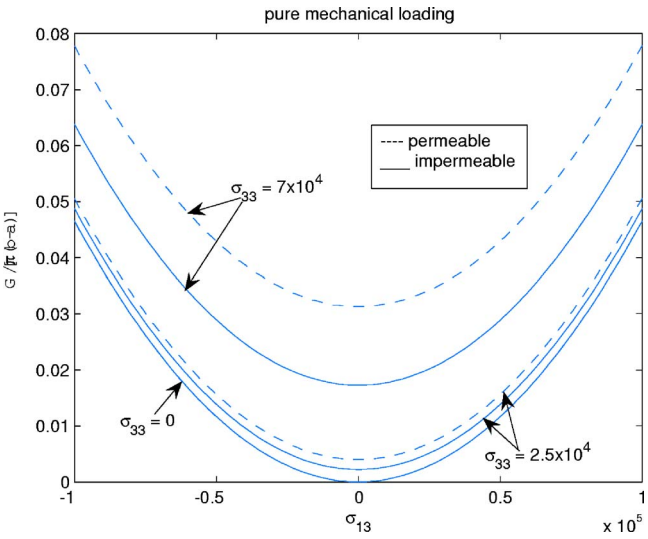

Fig. 6 Energy release rate versus σ_{13} for a given σ_{33}

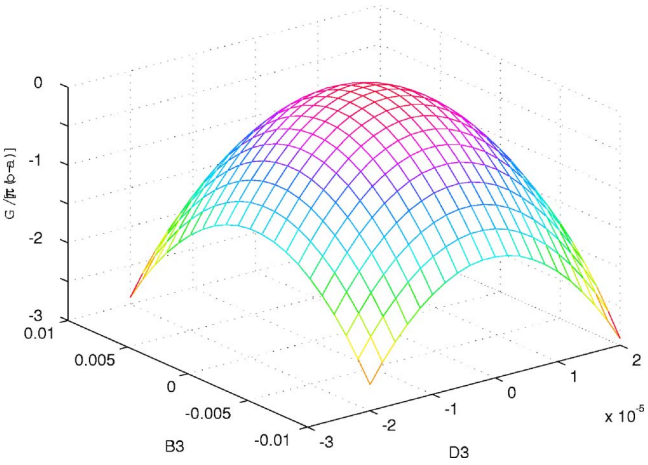

Fig. 7 Energy release rate under pure electric and magnetic applied loading

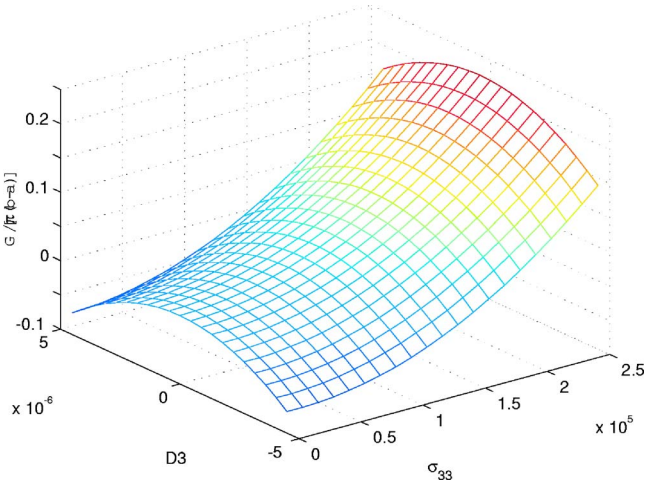

Fig. 9 Energy release rate under combined mechanical σ_{33} and electrical D_3 loading

10. Particularly in Fig. 10, when $\sigma_{33}<2.8\times10^5$, the G is bigger for $B_3=0.25\times10^{-2}$ than for $B_3=0.5\times10^{-2}$. But the trend reverses when $\sigma_{33}>2.8\times10^5$.

One can further see that the surface of G is not symmetric with respect to the plane $D_3=0$ or $B_3=0$, as shown in Figs. 9 and 11. It is possible that the value of G with $D_3=0$ or $B_3=0$ is smaller than the value of G with $D_3>0$ or $B_3>0$ when σ_{33} reaches a certain value. This result can be more explicitly observed from the results in Fig. 11. Therefore, an important conclusion which can be drawn here is that the applied D_3 and B_3 do not always contribute a negative value to the energy release rate G when an applied mechanical loading σ_{33} is also present. This conclusion further suggests that the applied electric and magnetic loading does not always retard the propagation of an interface crack. Instead, under certain conditions of the applied mechanical loading, σ_{33}, they may actually speed the propagation of an interface crack.

Figures 13–15 study the influence of D_3 or B_3 on the energy release rate, G, under mechanical applied shear loading σ_{13}. Figure 13 is the variation of G versus any combination of (σ_{13},D_3). One can see that the surface of G is symmetric both with respect to the axis $\sigma_{13}=0$ and the $D_3=0$. This observation indicates that the direction of D_3 has no effect on the energy release rate G if the applied loading is only σ_{13} and $B_3=0$. This result can be easily

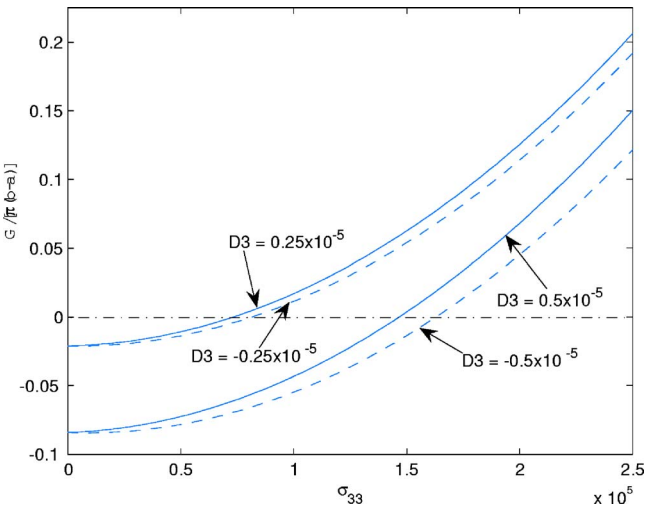

Fig. 8 Energy release rate versus σ_{33} for a given D_3

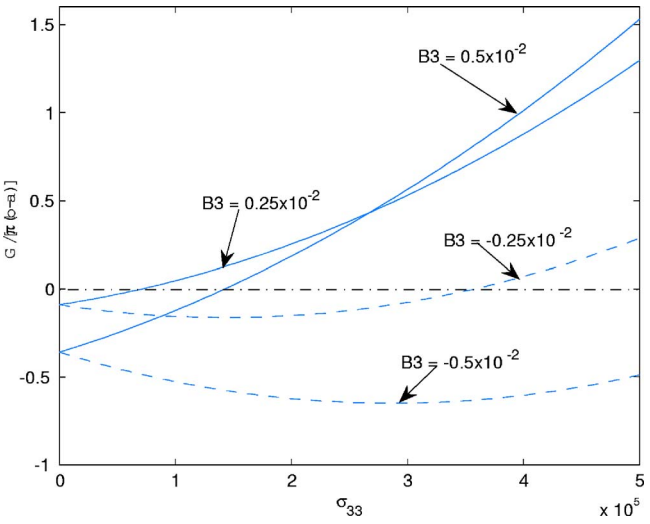

Fig. 10 Energy release rate versus σ_{33} for a given B_3

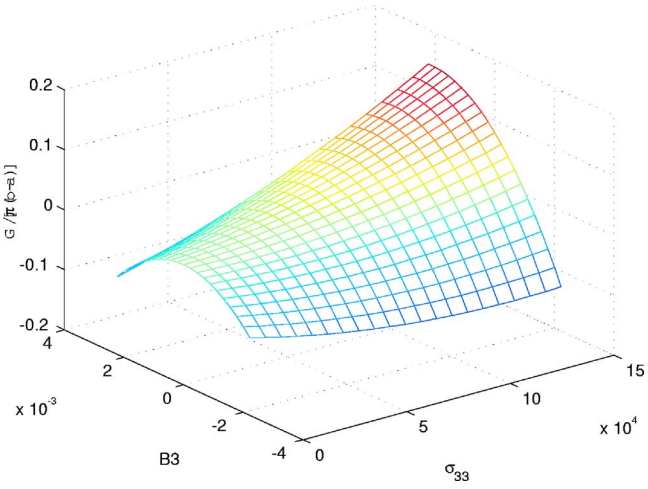

Fig. 11 Energy release rate under combined mechanical σ_{33} and magnetic B_3 loading

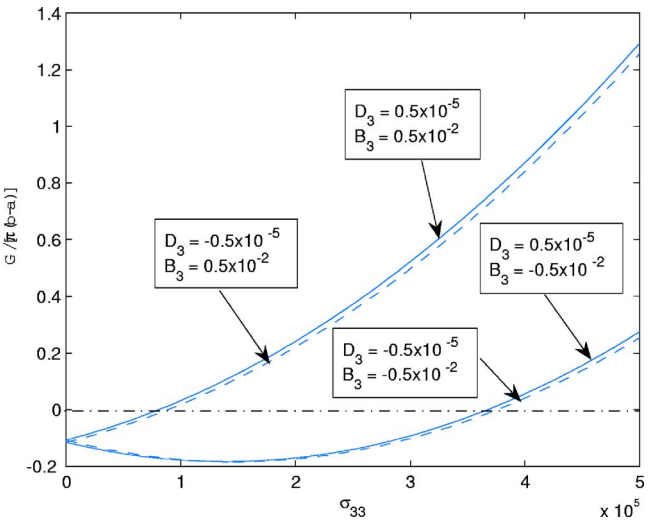

Fig. 12 Energy release rate under loading σ_{33} for a given $(\pm B_3, \pm D_3)$

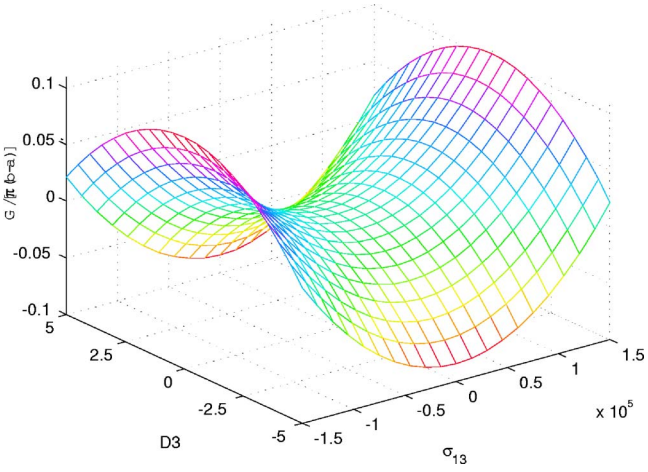

Fig. 13 Energy release rate under loading σ_{13} and D_3

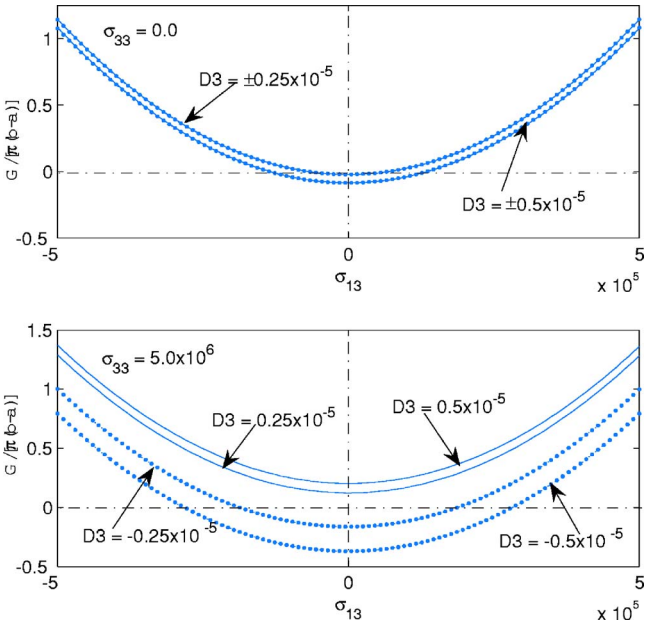

Fig. 14 Variation of energy release rate versus σ_{13}: top for a given D_3 only; bottom for a given pair (D_3, σ_{33})

seen from the top graphic in Fig. 14. A similar tendency can also be found for the case when only σ_{13} and B_3 are applied, as shown in the top graph of Fig. 15. As a comparison, the results with $\sigma_{33} \neq 0$ are also plotted at the bottom of Figs. 14 and 15. The results in Figs. 13–15 also show that the applied electric (D_3) or/and magnetic (B_3) field(s) usually retard(s) the propagation of an interface crack when the applied mechanical loading is only the shear loading σ_{13}.

Figures 16 and 17 plot the results of the energy release rate G under both tensile and shear in-plane applied loading. Figure 16 is the G versus $(\sigma_{33}, \sigma_{13})$ under simultaneously given D_3 and B_3, and Fig. 17 is a particular case for $\sigma_{13} = \pm 3.25 \times 10^5$. These results demonstrate that different combinations of the directions of D_3 and B_3 produce different results of the energy release rate G. For a given σ_{33} and σ_{13}, there exist a direction for D_3 and B_3 that makes the G maximum. One can also see that for any given D_3 and B_3, the G is symmetric with respect to σ_{13}. This observation, together with similar observations in Figs. 13 and 15, show that the direction of in-plane shear loading σ_{13} has no effect on G. Although when individually applied with $\sigma_{33}=0$, the direction of D_3 or B_3 does not affect the G as shown in Fig. 13, the top of Fig. 14, and the top of Fig. 15, the directions of D_3 or B_3 do have effects on the G when they are applied together as clearly shown in Fig. 16 and 17, say, values are different when directions of D_3 and B_3 are different with $\sigma_{33}=0$ and $\sigma_{13} = \pm 3.25 \times 10^5$, as depicted in Fig. 17.

5 Conclusions

Four possible singularities of the form $r^{-(1/2)\pm\epsilon_1}$ and $r^{-(1/2)\pm i\epsilon_2}$ exist for the fields around an interface crack tip in dissimilar PEMO—elastic bimaterial media. The bimaterial parameters ϵ_1 and ϵ_2 are proven to be real numbers for practical materials. The electric—magnetic field inside the crack is solved by finding the stationary point of the saddle surface of the energy release rate with respect to the electromagnetic field inside the crack. The energy release rate, G, can be expressed in compact form both for impermeable and permeable interface cracks. The value of G increases as the bimaterial parameter c_2 (defined by Eq. (102) in Appendix B) increases. When the only applied mechanical loading is σ_{13} (in-plane shear), the directions of separately applied D_3

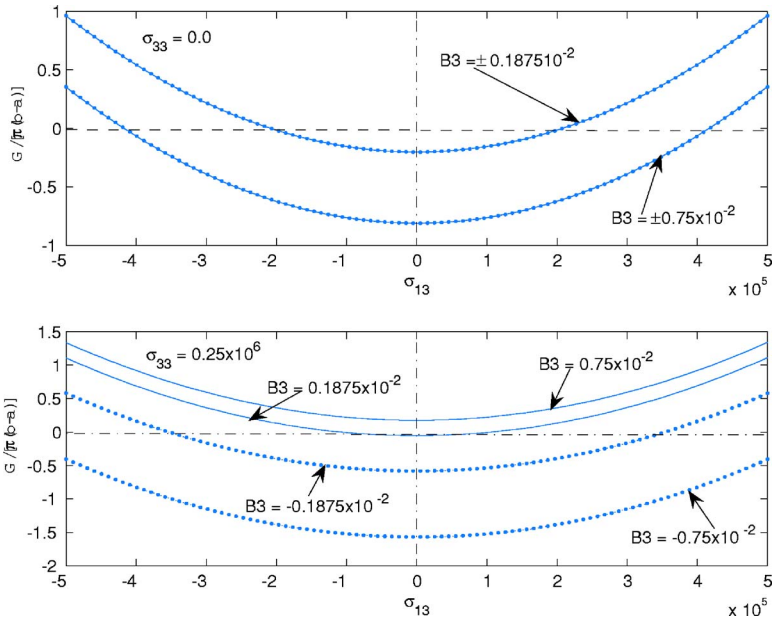

Fig. 15 Variation of energy release rate versus σ_{13}: top for a given B_3 only; bottom for a given pair (B_3, σ_{33})

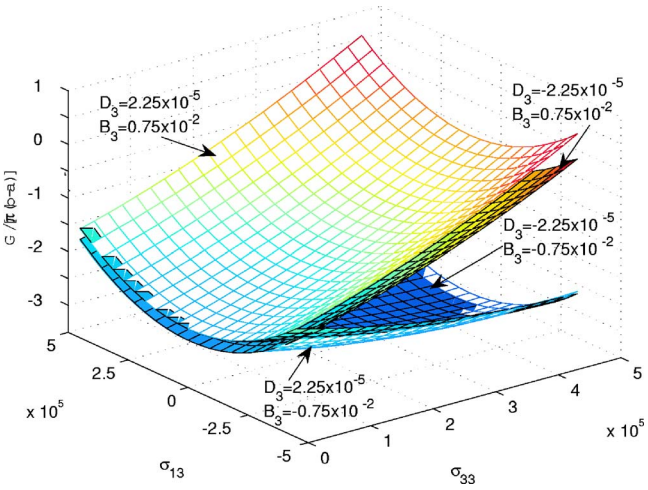

Fig. 16 Variation of energy release rate versus $(\sigma_{33}, \sigma_{13})$ for a given (D_3, B_3)

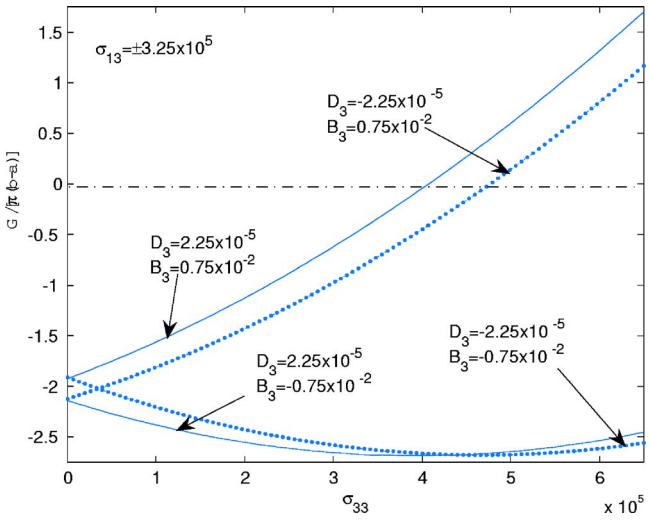

Fig. 17 Variation of energy release rate versus σ_{33} for a given (σ_{13}, D_3, B_3)

and B_3 do not affect the value of G while the directions of simultaneously applied D_3 and B_3 do. But the directions of applied D_3 and B_3 always have influences on the value of energy release rate G if the applied mechanical loading involves σ_{33} (tension). There exist a pair of directions of D_3 and B_3 which makes the G the maximum for each given mechanical loading. Pure applied electric–magnetic loading lowers G and therefore is expected to retard the propagation of an interface crack. However, the electric–magnetic loading does not always retard the propagation of an interface crack when the mechanically applied loading includes σ_{33} (tension). They can also foster the propagation of an interface crack if the applied mechanical loading reaches a certain value. The results or observations in this paper are still fundamental for the investigation of dissimilar piezoelectromagneto–elastic bimaterial solids. There are still more studies needed on this subject, such as in finding the criteria for the propagation of an interface crack, in understanding how the electric and magnetic fields inside an interface crack would interfere with the measured signals in broad band probes, etc. Nevertheless, the results in the current study may serve as a basis for more complex investigations.

Acknowledgment

The financial support of the Office of Naval Research, Grant No. N00014-90-J-1995, and the interest and encouragement of the Grant Monitor, Dr. Y. D. S. Rajapakse, are both gratefully acknowledged.

Appendix A. Bimaterial Constants: Real ϵ_1, ϵ_2

To ensure a nontrivial solution for the homogeneous Hilbert Eq. (50), the following condition should be satisfied

$$\|N + e^{2\pi i\delta}\bar{N}\| = \|N - e^{2\pi\epsilon}\bar{N}\| = 0 \tag{98}$$

where $\delta = 1/2 - i\epsilon$. Substituting Eq. $(45)_2$ into Eq. (98) leads to

$$\|W + i\beta D\| = 0 \tag{99}$$

where

$$\beta = \frac{e^{2\pi\epsilon} - 1}{e^{2\pi\epsilon} + 1}, \quad \text{or} \quad \beta = \tanh(\pi\epsilon) \tag{100}$$

Since N is Hermitian, from the definition of Eq. (100) one may easily see that if β and $\bar{\beta}$ are roots of Eq. (99), so are $-\beta$ and $-\bar{\beta}$. Therefore, Eq. (99) should have the form

$$p(i\beta) = (i\beta)^4 + 2c_2(i\beta)^2 + c_4 = 0 \tag{101}$$

where

$$2c_2 = -\tfrac{1}{2}\mathrm{tr}(D^{-1}W)^2, \quad c_4 = \|(D^{-1}W)\| \tag{102}$$

Then, the roots of Eq. (101) can be expressed as follows

$$\beta_{1,2} = \pm\sqrt{c_2 + \sqrt{(c_2)^2 - c_4}}$$

$$\beta_{3,4} = \pm\sqrt{c_2 - \sqrt{(c_2)^2 - c_4}} \tag{103}$$

These βs can be verified as real numbers. Actually, for the square matrices D and W, one has $\|(D^{-1}W)\| = \|D^{-1}\| \times \|W\|$, but $\|W\| \geqslant 0$, a property of an anti-symmetric matrix of even order, and $\|D^{-1}\| \geqslant 0$, a result from Eq. (27) and (28). So $c_4 = \|(D^{-1}W)\| \geqslant 0$. Mathematically, $(c_2)^2$ could be less than c_4. But for practical PEMO—elastic bimaterials, if $(c_2)^2 < c_4$, then $c_2 \pm \sqrt{(c_2)^2 - c_4}$ would be complex numbers with nonzero real and imaginary parts. Consequently, all the βs would be complex numbers, as would all the ϵs. This would contradict the fact in the literature that at least two singularities should have the form of $r^{-1/2\pm i\tilde{\epsilon}}$ with real $\tilde{\epsilon}$, in the case of bimedia with no piezoelectric/piezomagnetic material properties. Hence $(c_2)^2 \geqslant c_4$, as shown in Table 2. Further, the c_2 also should not be less than zero for practical materials. If c_2 is less than zero, one could find that all the βs in Eq. (103) would be pure imaginary numbers. Then from Eq. (100), all the singularities would have the form $r^{-1/2\pm\hat{\epsilon}}$ with real $\hat{\epsilon}$. This assertion would also contradict the fact that for bimedia with no piezoelectric/piezomagnetic material properties, at least two singularities have the form of $r^{-1/2\pm i\tilde{\epsilon}}$ with real $\tilde{\epsilon}$. Hence, $c_2 \geqslant 0$ (also shown in Table 2 for practical PEMO—elastic bimaterials). Therefore, one can conclude that the $\beta_{1,2}$, $\beta_{3,4}$ are real numbers, and so are the ϵ_1 and ϵ_2. One may realize that c_2 and c_4 are simultaneously equal to zero if W is null, a special case similar to the one discussed by Qu and Li [13] for conventional dissimilar anisotropic bimaterials.

Appendix B. Contour Integral for $\Phi(z)'$ and $\Phi(z)$

The method used here can be viewed as the generalization of the technique in Muskhelishvili (Ref. [28] Secs. 110, 70), which is for a single equation. Let γ be a contour which includes the arc $\overline{ab}$, and let this contour shrink into the arc $\overline{ab}$ (Fig. 1), then for the $q(x_1)$ constant

$$\int_\gamma \frac{[X(\xi)]^{-1}N^{-1}}{\xi - z}d\xi = \int_{\overline{ab}} \frac{[X_+(x_1)]^{-1}N^{-1}}{x_1 - z}dt + \int_{\overline{ba}} \frac{[X_-(x_1)]^{-1}\bar{N}}{x_1 - z}dx_1$$

$$= \int_{\overline{ab}} \frac{[X_+(x_1)]^{-1}N^{-1}}{x_1 - z}dx_1 - \int_{\overline{ab}} \frac{[X_-(x_1)]^{-1}N^{-1}}{x_1 - z}dx_1 \tag{104}$$

From Eq. (50), one can have

$$X_-(x_1) = -\bar{N}^{-1}NX_+(x_1), \quad a < x_1 < b \tag{105}$$

Substituting Eq. (105) into Eq. (104) leads to

$$\int_\gamma \frac{[X(\xi)]^{-1}N^{-1}}{\xi - z}d\xi = \int_{\overline{ab}} \frac{[X_+(x_1)]^{-1}N^{-1}[I + \bar{N}N^{-1}]}{x_1 - z}dx_1 \tag{106}$$

Then,

$$\int_{\overline{ab}} \frac{[X_+(x_1)]^{-1}N^{-1}}{x_1 - z}dx_1 = \int_\gamma \frac{[X(\xi)]^{-1}N^{-1}[I + \bar{N}N^{-1}]^{-1}}{\xi - z}d\xi$$

$$= \int_\gamma \frac{[X(\xi)]^{-1}[N + \bar{N}]^{-1}}{\xi - z}d\xi \tag{107}$$

but

$$J = \frac{1}{2\pi i}\int_\gamma \frac{[X(\xi)]^{-1}[N + \bar{N}]^{-1}}{\xi - z}d\xi = \{X(z)^{-1}v - [\Xi + \Pi]\}v^{-1}[N + \bar{N}]^{-1} \tag{108}$$

where Ξ and Π are defined in Eq. (64). Therefore

$$\Phi'(z) = \frac{X(z)}{2\pi} \times 2\pi i J = v\left\{I - \frac{\Delta(z;\epsilon_1,\epsilon_2)}{\sqrt{(z-a)(z-b)}}[\Xi + \Pi]\right\}v^{-1}[N + \bar{N}]^{-1}ip \tag{109}$$

References

[1] Alshits, V. I., Darinskii, A. N., and Lothe, J., 1992, "On the Existence of Surface Waves in Half-Infinite Anisotropic Elastic Media With Piezoelectric and Piezomagnetic Properties," Wave Motion, **16**, pp. 265–283.

[2] Benveniste, Y., 1995, "Magnetoelectric Effect in Fibrous Composites With Piezoelectric and Piezomagnetic Phases," Phys. Rev. B, **51**(22), pp. 16424–16427.

[3] Chung, M. Y., and Ting, T. C. T., 1995, "The Green Function for a Piezoelectric Piezomagnetic Anisotropic Elastic Medium With an Elliptic Hole or Rigid Inclusion," Philos. Mag. Lett., **72**(6), pp. 405–410.

[4] Pan, E., 2002, "Three-Dimensional Green's Functions in Anisotropic Magneto-Electro-Elastic Bimaterials," J. Math. Phys., **53**, pp. 815–838.

[5] Bichurin, M. I., Filippov, D. A., Petrov, V. M., Laletsin, V. M., and Paddubnaya, N., 2003, "Resonance Magnetoelectric Effect in Layered Magnetostrictive-Piezoelectric Composites," Phys. Rev. B, **68**, pp. 132408-1–132408-4.

[6] Williams, M. L., 1959, "The Stress Around a Fault or Crack in Dissimilar Media," Bull. Seismol. Soc. Am., **49**(2), pp. 199–204.

[7] Erdogan, F., 1963, "The Stress Distribution in a Nonhomogeneous Elastic Plane With Cracks," J. Appl. Mech., **85**, pp. 232–236.

[8] England, A. H., 1965, "A Crack Between Dissimilar Media," J. Appl. Mech., **32**, pp. 400–402.

[9] Rice, J. R., and Sih, G. C., 1965, "Plane Problems of Cracks in Dissimilar Media," J. Appl. Mech., **32**, pp. 418–423.

[10] Clements, D. L., 1971, "A Crack Between Dissimilar Anisotropic Media," Int. J. Eng. Sci., **9**, pp. 257–265.

[11] Willis, R. J., 1971, "Fracture Mechanics of Interfacial Cracks," J. Mech. Phys. Solids, **19**, pp. 353–368.

[12] Suo, Z., and Hutchinson, J. W., 1990, "Interface Crack Between Two Elastic Layers," Int. J. Fract., **43**, pp. 1–18.

[13] Qu, J., and Li, Q. Q., 1991, "Interfacial Dislocation and Its Applications to Interface Cracks in Anisotropic Bimaterials," J. Elast., **26**, pp. 169–195.

[14] McMeeking, R. M., 1989, "Electrostrictive Forces Near Crack Like Flaws," J. Appl. Math. Phys., **40**, pp. 615–627.

[15] Kuo, C.-M., and Barnett, D. M., 1991, *Modern Theory of Anisotropic Elasticity and Applications* (SIAM Proceeding Series), J. J. Wu, T. C. T. Ting, and D. M. Barnett eds., SIAM, Philadelphia, PA, pp. 33–50.

[16] Suo, Z., Kuo, C.-M., and Willis, R. J., 1992, "Fracture Mechanics for Piezoelectric Ceramics," J. Mech. Phys. Solids, **40**, pp. 739–765.

[17] Sih, G. C., and Song, Z. F., 2003, "Magnetic and Electric Poling Effects Associated With Crack Growth in $BaTiO_3$–$CoFe_2O_4$ Composites," Theor. Appl. Fract. Mech., **39**, pp. 209–227.

[18] Song, Z. F., and Sih, G. C., 2003, "Crack Initiation Behavior in Magneto-Electro-Elastic Composite Under In-plane Deformation," Theor. Appl. Fract. Mech., **39**, pp. 189–207.

[19] Gao, C. F., Kessler, H., and Balke, H., 2003, "Crack Problems in Magneto-electroelastic Solids—Part I: Exact Solution of a Crack," Int. J. Eng. Sci., **41**, pp. 969–981.

[20] Gao, C. F., Tong, P., and Zhang, T.-Y., 2003, "Interfacial Crack Problems in Magneto-Electric Solids," Int. J. Eng. Sci., **41**(18), pp. 2105–2121.

[21] Stroh, A. N., 1958, "Dislocations and Cracks in Anisotropic Elasticity," Philos. Mag., **8**(3), pp. 625–646.

[22] Barnett, D. M., and Lothe, J., 1975, "Dislocations and Line Charges in Anisotropic Piezoelectric Insulators," Phys. Status Solidi B, **67**, p. 105.
[23] Li, R., and Kardomateas, G. A., 2006, "Mode III Interface Crack of Piezo-Electro-Magneto-Elastic Dissimilar Bi-material Composites," J. Appl. Mech., **73**(2), pp. 220–227.
[24] Lothe, J., and Barnett, D. M., 1976, "Integral Formalism for Surface Waves in Piezoelectric Crystals. Existence Considerations," J. Appl. Phys., **47**(5), pp. 1799–1807.
[25] Barnett, D. M., and Lothe, J., 1973, "Synthesis of Sextic and the Integral Formalism for Dislocations, Greens Functions, and Surface Waves in Anisotropic Elastic Solids," Phys. Norv., **7**(1), pp. 13–19.
[26] Li, R., and Kardomateas, G. A., 2005, "A Solution to the Thermoelastic Interface Delamination Branching Behavior for Dissimilar Anisotropic Bi-material Media," Int. J. Solids Struct., in Press.
[27] Rudin, W., 1987, *Real and Complex Analysis*, McGraw-Hill, New York.
[28] Muskhelishvili, N. I., 1992, *Singular Integral Equations*, Dover, New York.